ISSN 1674-1056
http://cpb.iphy.ac.cn
http://iopscience.iop.org/cpb
中国物理 B
Chinese Physics
中国物理
Chinese Physics B

Supercontinuum manipulation based on the influence of chirp on soliton spectral tunneling

SaiLi Zhao(赵赛丽), Huan Yang(杨华), YiLin Zhao(赵奕霖), YuZhe Xiao(肖宇哲)

Citation: Chin. Phys. B . 2018, 27(11): 114219. **doi:** 10.1088/1674-1056/27/114219
Journal homepage: http://cpb.iphy.ac.cn; http://iopscience.iop.org/cpb

What follows is a list of articles you may be interested in

Intense supercontinuum generation in the near-ultraviolet range from a 400-nm femtosecond laser filament array in fused silica

Dongwei Li(李东伟), Lanzhi Zhang(张兰芝), Saba Zafar, He Song(宋鹤), Zuoqiang Hao(郝作强), Tingting Xi(奚婷婷), Xun Gao(高勋), Jingquan Lin(林景全)

Chin. Phys. B . 2017, 26(7): 074213. **doi:** 10.1088/1674-1056/26/7/074213

Numerical investigation on broadband mid-infrared supercontinuum generation in chalcogenide suspended-core fibers

Kundong Mo(莫坤东), Bo Zhai(翟波), Jianfeng Li(李剑峰), E Coscelli, F Poli, A Cucinotta, S Selleri, Chen Wei(韦晨), Yong Liu(刘永)

Chin. Phys. B . 2017, 26(5): 054216. **doi:** 10.1088/1674-1056/26/5/054216

Frequency-stabilized Yb:fiber comb with a tapered single-mode fiber

Yang Xie(谢阳), Hai-Nian Han(韩海年), Long Zhang(张龙), Zi-Jiao Yu(于子蛟), Zheng Zhu(朱政), Lei Hou(侯磊), Li-Hui Pang(庞利辉), Zhi-Yi Wei(魏志义)

Chin. Phys. B . 2016, 25(4): 044208. **doi:** 10.1088/1674-1056/25/4/044208

Different supercontinuum generation processes in photonic crystal fibers pumped with a 1064-nm picosecond pulse

Chen Hong-Wei, Jin Ai-Jun, Chen Sheng-Ping, Hou Jing, Lu Qi-Sheng

Chin. Phys. B . 2013, 22(8): 084205. **doi:** 10.1088/1674-1056/22/8/084205

Supercontinuum generated in all-normal dispersion photonic crystal fibers with picosecond pump pulses

Li Pan, Shi Lei, Mao Qing-He

Chin. Phys. B . 2013, 22(7): 074204. **doi:** 10.1088/1674-1056/22/7/074204

Supercontinuum manipulation based on the influence of chirp on soliton spectral tunneling*

Saili Zhao(赵赛丽)[1,2,†], Huan Yang(杨华)[1,3,‡], Yilin Zhao(赵奕霖)[1], and Yuzhe Xiao(肖宇哲)[4]

[1] College of Information Science and Engineering, Key Laboratory for Micro/Nano Optoelectronic Devices of Ministry of Education, Hunan University, Changsha 410082, China

[2] Electrical Engineering Department, University of California, Los Angeles, California 90095, USA

[3] Synergetic Innovation Center for Quantum Effects and Application, Hunan Normal University, Changsha 410082, China

[4] Department of Electrical Engineering, University of Wisconsin Madison, Madison, Wisconsin 53706, USA

(Received 17 April 2018; revised manuscript received 7 August 2018; published online 19 October 2018)

The soliton spectral tunneling (SST) effect, as a soliton spectral switching phenomenon, enables a soliton to tunnel through a spectrally limited regime of normal dispersion in the fiber with multiple zero dispersion wavelengths (ZDWs). Since initial chirp can affect the behavior of pulse evolution, we numerically study the influence of chirp on the SST in the process of supercontinuum (SC) occurring in a photonic crystal fiber (PCF) with three ZDWs. The linear chirp is imposed by a phase modulation of input pulse while maintaining a constant pulse duration. Interestingly, it is found that the spectral range and flatness can be flexibly tuned by adjusting the initial chirp value. More specifically, positive chirp facilitates soliton self-frequency shifting (SSFS), making the soliton quickly transfer from one anomalous dispersion regime to another accompanied by the generation of dispersive waves (DWs). In this case, the SST effect further expands the spectral range by enhancing both the red-shift of the fundamental soliton and the blue-shift of DWs, thus generating a broader SC. However, negative chirp suppresses the SST effect, resulting in a smoother SC at the expense of bandwidth. Therefore, the findings in this work provide interesting results relating to the influence of initial chirp on the SST to generate a considerably smoother and broader SC, which is extremely useful in many applications, such as wavelength conversion and SC generation.

Keywords: soliton spectral tunneling, supercontinuum generation, chirp

PACS: 42.81.–i, 42.81.Dp, 42.65.–k **DOI:** 10.1088/1674-1056/27/11/114219

1. Introduction

Optical solitons have been a hot topic of research since they are regarded as good information carriers for long-distance communication and all-optical ultrafast switching devices.[1] The formation of optical solitons results from the delicate balance between dispersive broadening and nonlinear self-compression.[1–3] Generally speaking, optical solitons can only exist in the anomalous group velocity dispersion (GVD) regime.[3,4] However, soliton self-frequency shifting (SSFS) gives rise to the change because of the existence of multiple zero dispersion wavelengths (ZDWs) in the fiber. In addition, there have been many studies demonstrating that the SSFS enables a soliton to tunnel through a spectrally limited normal GVD regime, which is referred to as soliton spectral tunneling (SST).[5–7]

The SST effect happens when Raman-induced SSFS continuously transfers soliton energy from one anomalous dispersion regime to another as the soliton propagates through the fiber.[8,9] More fundamentally, the SST effect requires a normal GVD regime to act as a potential barrier sandwiched between two anomalous ones. Such characteristics are difficult to achieve in conventional fibers, but can be easily realized in photonic crystal fibers (PCFs) because their mode dispersion relates to their geometric features.[3,5,10] By adjusting the geometry of the PCF, the dispersion profile with multiple ZDWs can be obtained in practice.[11] As is well known, dispersive waves (DWs) as soliton-induced optical Cherenkov radiation are resonant waves meeting the phase matching (PM) condition with the launched soliton.[12–14] Simultaneously, DWs play a crucial role in generating octaves-panning supercontinuum (SC) in fiber structures since they dominate the blue-shifted edge of the spectrum while Raman-induced SSFS results in the red-shifted edge. Such a mechanism has been theoretically and experimentally demonstrated in the PCF with two ZDWs.[15,16] However, when soliton-induced DWs are obtained in one of the anomalous dispersion regimes in the PCF with multiple ZDWs, the SST effect can transform the DWs into soliton waves. Therefore, the SST effect is also considered as a sort of drive for the generation of soliton-induced DWs since the transferred soliton is phase-matched to the launched soliton.[17,18] What is more, the group-velocity matching (GVM) between the launched soliton and the trans-

*Project supported by the National Natural Science Foundation of China (Grant Nos. 61275137 and 61571186) and the Natural Science Foundation of Hunan Province, China (Grant No. 2018JJ2061).

†Corresponding author. E-mail: zhaosaili@hnu.edu.cn

‡Corresponding author. E-mail: huayang@hnu.edu.cn

© 2018 Chinese Physical Society and IOP Publishing Ltd

ferred soliton is another necessary condition for the emergence of the SST effect.[9,19] Previous papers mainly focused on the SST effect as a spectral switching phenomenon occurring in the fiber with different dispersion profiles.[17,19–21] For example, Poletti *et al.* numerically demonstrated the SST effect in an index-guiding holey fiber with a tunable GVD barrier over a wide wavelength span.[19] In another work, Wang *et al.* showed a cascaded SST effect in segmented fibers with engineered dispersion, which can lead the soliton pulse to transfer over a wide wavelength span.[20] There have been many studies indicating that initial chirp can exert an influence on both fundamental solitons and DWs in SC generation.[21–25] For example, Lei *et al.* showed how to conveniently and efficiently manipulate the DW generation by controlling the prechirp of the input pulse.[14] In addition, Cheng *et al.* proved that there exists an optimal positive chirp maximizing the spectral bandwidth.[26] However, there are few studies focusing on the influence of initial chirp on the SST process in the fiber. In the present work, we study the influence of initial chirp on the SST in the process of SC occurring in a PCF with three ZDWs. Because the interaction between DWs and Raman solitons plays a key role in the SST effect, it is meaningful to investigate how to manipulate the SC when considering the effect of chirp on the SST.

The rest of this paper is organized as follows. In Section 2, the basic propagation model for the input pulse is proposed, which includes linear and nonlinear effects. At the same time, the PM condition is illustrated at the pump wavelength. Detailed numerical simulations about the influence of positive chirp, zero chirp, and negative chirp on the SST effect in SC generation are presented in Section 3. Finally, numerical simulation results are summarized briefly in Section 4.

2. Numerical model for ultrashort pulse propagation in the PCF

Propagation of ultrashort pulses in a PCF with three ZDWs can be described by the generalized nonlinear Schrödinger equation (GNLSE), which includes dispersion effects and nonlinear effects such as self-phase modulation (SPM), self-steepening, and stimulated Raman scattering (SRS). The GNLSE can be expressed as[3]

$$\frac{\partial A(z,T)}{\partial z} = \sum_{k\geq 2} \frac{\mathrm{i}^{k-1}\beta_k}{k!}\frac{\partial^k A}{\partial T^k} + \mathrm{i}\gamma\left(1+\frac{\mathrm{i}}{\omega_0}\frac{\partial}{\partial T}\right) \times \left[A(z,T)\int_{-\infty}^{+\infty} R(T')\left|A(z,T-T')\right|^2 \mathrm{d}T'\right], \tag{1}$$

where $A(z,T)$ is the complex slowly varying amplitude of the light field in the reference frame moving with the group velocity of the input pulse, z is the transmission distance, T is the time parameter, γ is the nonlinear coefficient, $R(T)$ is the nonlinear response function including the Kerr response and Raman response, and β_k is the dispersion coefficient of the k-th order at the central frequency ω_0. Note that even with the slowly varying envelope approximation, the GNLSE has been shown to accurately predict the ultra-short pulse behavior down to a few cycles.[27] Besides, loss is neglected here since a relatively short propagation length is considered in the PCF. The split-step Fourier method with adaptive step size control is adopted to solve the GNLSE. In this method, the linear and nonlinear terms on the right-hand side of equation (1) are integrated separately, and the results are combined to construct the solution to the full problem. The linear term of equation (1) is solved in the frequency domain. The time derivative in the nonlinear term is regarded as a perturbation, and we use a second-order Runge–Kutta method to carry out the integration of the nonlinear step. The convolution integral between the field intensity and the delayed Raman response is calculated as a simple product in the frequency domain. Both real and imaginary parts of the Raman susceptibility are included.

The investigation on the dependence of SC characteristics on input chirp has been carried out for two different cases, both considering anomalous GVD regime pumping under the typical femtosecond pumping conditions. In the first case, the linear chirp is obtained by imposing a quadratic spectral phase on the input pulse while maintaining a constant pulse bandwidth. In this case, the pulse energy remains fixed, but increased chirp is associated with an increased pulse duration and reduced peak power.[28,29] In the second case, the linear chirp is imposed by a phase modulation of the input pulse while maintaining a constant pulse duration.[30] In this paper, the linear chirp is added in the form of the second case. Therefore, the prechirped input pulse with a hyperbolic secant shape is as follows:

$$A(0,T) = \sqrt{P_0}\,\mathrm{sech}(T/T_0)\exp(-\mathrm{i}CT^2/2T_0^2), \tag{2}$$

where P_0 and C are the peak power and initial chirp parameter, respectively. The formation of a soliton is expected for small values of $|C|$ since solitons are generally stable under weak perturbations. However, a soliton is destroyed if $|C|$ exceeds the related critical value, which can be theoretically obtained by the inverse scattering method.[3,31] In this paper, the initial chirp parameters are all below the critical value.

The parameters of input pulse are chosen as follows: initial pulse width $T_0 = 50$ fs, central wavelength $\lambda_0 = 804$ nm, and peak power $P_0 = 15$ kW. It is important to ensure that the time window is sufficiently large to avoid the cyclic wrapping of the temporal envelope with propagation. The longitudinal step size is also important, and must be sufficiently small to accurately model the nonlinear and dispersive interactions as

the field propagates. Here, we choose 3000 as the longitudinal step number and $320T_0 = 16$ ps as the temporal window width. The number of discretization points is 2^{12}. Therefore, the temporal resolution is $16\ \text{ps}/2^{12} \approx 3.9$ fs.

The PCF with three ZDWs has a strong dispersion effect, and therefore multiple high-order dispersion needs to be considered.[32] The dispersion curve and group delay curve of the PCF considered in this study as a function of wavelength are plotted in Fig. 1(a). The three ZDWs (771 nm, 924 nm, and 1014 nm) divide the entire spectrum into four regimes, namely, a short wavelength normal dispersion regime (R_1: $\lambda < 771$ nm), a short wavelength anomalous dispersion regime (R_2: $771\ \text{nm} \leq \lambda \leq 924$ nm), a long wavelength normal dispersion regime (R_3: $924\ \text{nm} \leq \lambda \leq 1014$ nm), and a long wavelength anomalous dispersion regime (R_4: $1014 < \lambda$ nm). Aside from the GVM between the launched soliton and the transferred soliton, the PM also needs to be considered for the emergence of the SST effect. The PM condition ($\Delta\beta = 0$) corresponding to the pump is demonstrated in Fig. 1(b), where $\Delta\beta$ presents the phase mismatch.

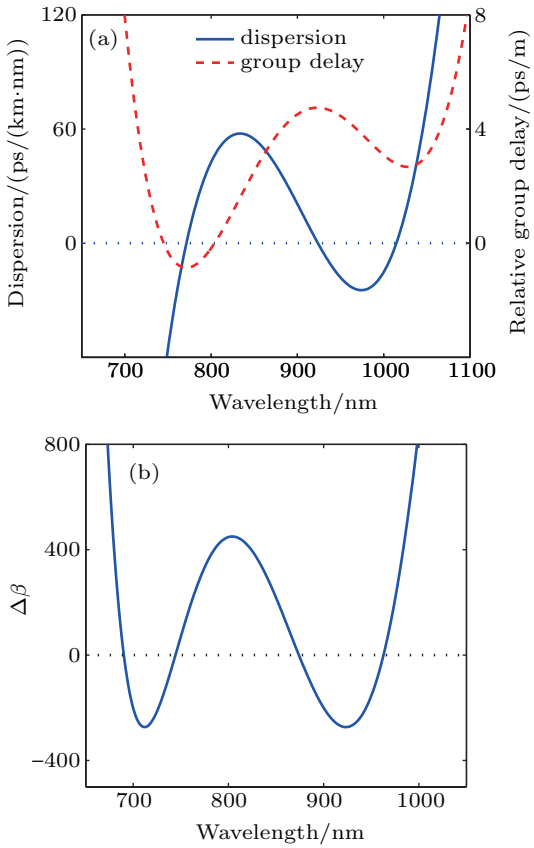


Fig. 1. (color online) (a) Dispersion (blue solid line) and related group delay (red dashed line), and (b) phase mismatch corresponding to the pump as a function of wavelength in the PCF with three ZDWs.

3. Numerical results and discussion

The output pulse shapes and corresponding temporal evolutions under the condition of different chirps in a 16 cm long PCF are plotted in Fig. 2. The SPM-induced chirp is positive, which can compress or broaden the pulse depending on how the input pulse is prechirped. In the case of zero chirp, SPM leads to temporal compression in the anomalous dispersion regime. For positive chirp, the compression strength is enhanced because of the superposition of two different positive chirps. In contrast to the zero chirp and positive chirp, the negative chirp makes the input pulse immediately broadened since its absolute value is much bigger than that of positive chirp from SPM. Shortly afterward, these pulses are all broadened due to the influence of GVD. Higher-order dispersion and Raman scattering are the two most significant effects that can break up the pulse into a series of fundamental solitons through soliton fission, which is accompanied by the emission of nonsoliton radiation. These ejected Raman solitons are obviously observed in the lower temporal evolution shown in Fig. 2, where the transmittal velocities gradually decrease while the related delays increase along the propagation. The first-ejected Raman soliton in the fission process experiences the greatest self-frequency downshifts from the pump. At the same time, the red-shift velocity of the generated soliton is gradually improved with the increase in the initial chirp value, where positive chirp facilitates the SSFS while negative chirp suppresses the SSFS. As a result, positive chirp makes fundamental soliton transfer from one anomalous dispersion regime (R_2) to another (R_4) at the largest rate. Accordingly, there are more blue-shifted DWs (B-DWs) radiated from fundamental solitons when meeting the PM condition. In addition, an interesting phenomenon is found: the output intensity of the first-ejected fundamental soliton with negative chirp is much higher than those with zero chirp and positive chirp. Such a phenomenon results from the fact that the fundamental soliton is tunneling from R_2 to R_4 and thereby compressing the temporal domain. In this case, the fundamental soliton transforms into the form of transferred DWs with a much higher intensity when transmitting through the long wavelength normal dispersion regime (R_3).

Figure 3 shows the output spectra and related spectral evolutions with different initial chirps. With the increase in propagation distance, the pulse evolution is divided into three stages, namely, the initial broadening stage, dramatic broadening stage, and saturation broadening stage. In the initial stage of spectral evolution, the SPM broadens the spectrum by generating new frequency components in the case of zero chirp. For the positive chirp, the spectrum is broadened to a larger degree due to the emergence of more new frequency components coming from the initial chirp. Meanwhile, for the negative chirp, the spectrum first undergoes narrowing and ultimately broadening.

In the case of an ultrashort pulse, because SPM is accompanied by other nonlinear effects such as SRS and four-

wave mixing (FWM), the spectrum can be extended to a very wide range so that the broadened spectrum can be regarded as SC. When the spectrum is broadened to the greatest degree by SPM, a series of fundamental solitons is ejected into R_2 because of Raman effects. Then the associated DWs are radiated from these ejected fundamental solitons because of higher-order dispersion effects. After initial fission, each fundamental soliton experiences SSFS to a longer wavelength. Since the SSFS resulting from Raman effects can go against the soliton recoiling effect, the fundamental soliton in R_2 can remain at its position while soliton coupling continuously takes place until the fundamental soliton is fully coupled into the adjacent channel to form a new soliton wave in R_4. The formation of a new fundamental soliton is based on the energy transferred from R_2 to R_4 when meeting GVM and PM conditions, which presents a soliton propagation process known as the SST effect. For positive chirp, the fundamental soliton is ejected at the fastest rate and undergoes the strongest SSFS, which facilitates it going through R_3. The above phenomena make the transferred soliton into R_4 have the largest red-shift and highest intensity. Meanwhile, the transferred soliton can radiate more energy to the corresponding DWs when meeting the PM condition. Therefore, the input pulse with positive chirp will be the first to complete the dramatic broadening stage and to reach the saturation broadening stage by enhancing both the red-shift of the fundamental soliton and the blue-shift of DWs. However, it is worth noting that the output spectrum in R_4 does not have the shape of a conventional fundamental soliton under the condition of negative chirp as shown in the upper panel of Fig. 3(a). From the lower panel of Fig. 3(a), we can see that the energy is being transferred from R_2 to R_4 at the output of the PCF, which indicates that a new soliton has not yet been fully formed in R_4. The above phenomenon is consistent with that shown in Fig. 2(a), where the first-ejected fundamental soliton exists in the form of the transferred DWs at the output of the PCF. When the pulse enters the saturation broadening stage, the initial chirp cannot affect the spectrum any longer. In order to better analyze the effect of initial chirp on SST in the SC generation, the output spectrograms with different initial chirps are demonstrated in detail.

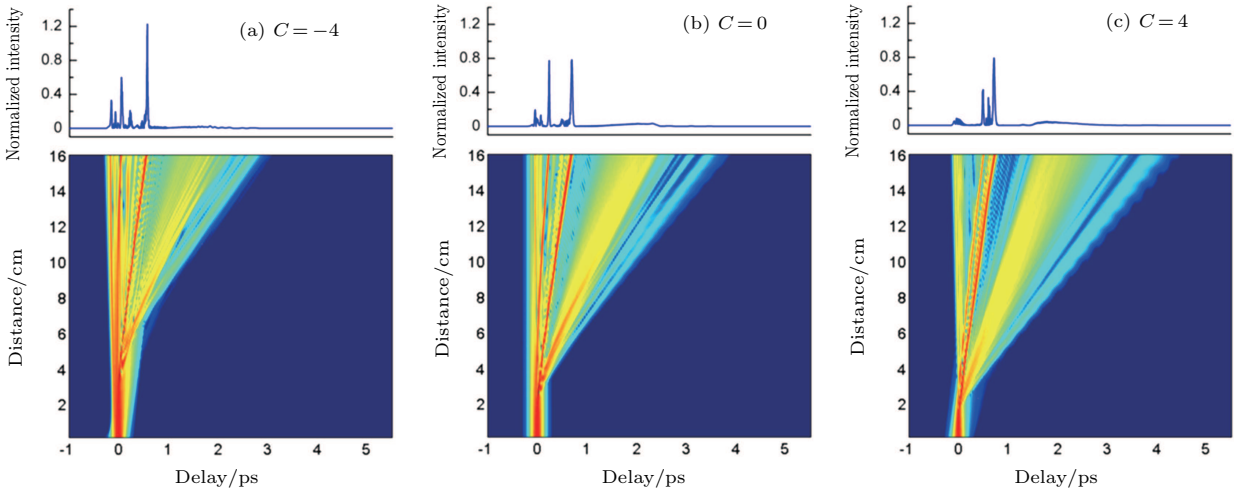


Fig. 2. (color online) Output pulse shapes (upper panels) and the corresponding temporal evolution as a function of fiber length (lower panels) under the condition of different initial chirps: (a) $C=-4$, (b) $C=0$, and (c) $C=4$.

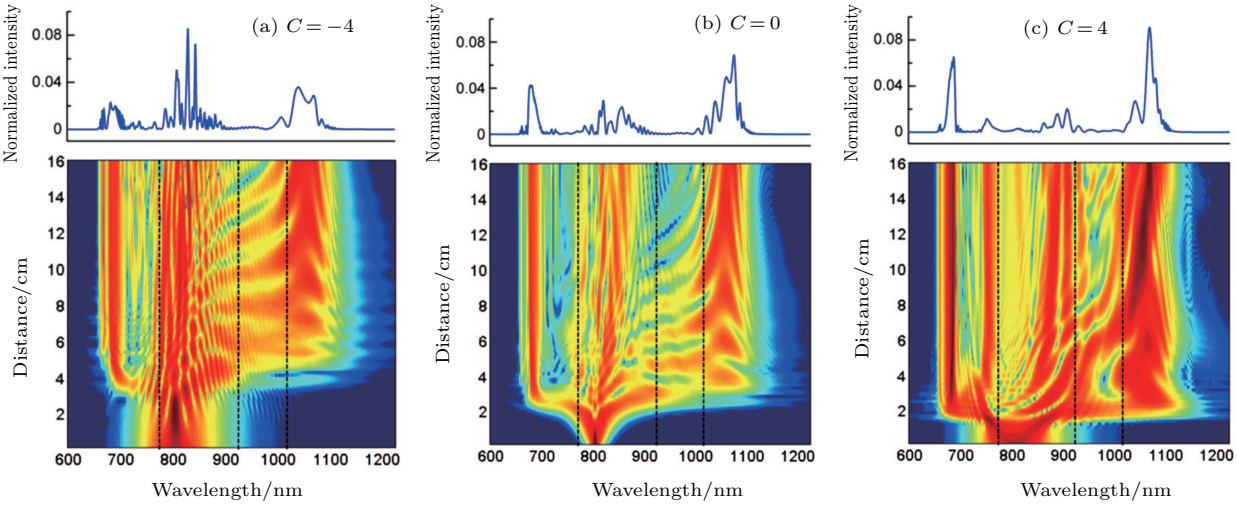


Fig. 3. (color online) Output spectra (upper panels) and the corresponding spectral evolution as a function of fiber length (lower panels) under the condition of different initial chirps: (a) $C=-4$, (b) $C=0$, and (c) $C=4$. The dashed vertical lines indicate the three ZDWs of the PCF.

Figure 4, including the spectrum (right vertical axis in the upper panel) and temporal intensity (left vertical axis in the lower panel) at the end of the PCF, shows the output spectrogram trajectories (basically irregular M-type), which are similar to the trace of group delay in Fig. 1(a). In contrast to the Z-shape output spectrogram trace in the PCF with two ZDWs, the M-shape spectrogram trace shows that the output spectrum owns more abundant frequency components. In the PCF with three ZDWs, the initial pump pulse is broken into a series of red-shifted fundamental solitons with different widths and peak intensities. The first-ejected fundamental soliton has a large spectral width and a higher peak power than the other solitons. Because of SSFS induced by intra-pulse Raman effects, the SST effect makes the energy of the first-ejected fundamental soliton transfer from R_2 to R_4 accompanied by the generation of related B-DWs when PM condition is met. With the increase in initial chirp, the intensity of the transferred soliton in R_4 and the related B-DWs in R_1 are enhanced; meanwhile, the red-shift of the transferred soliton and the blue-shift of the B-DWs are also enhanced, both of which make the SC expand to a much broader range. Because the red-shift rate of the fundamental soliton gradually decreases with a decreasing initial chirp, the first-ejected fundamental soliton is fully coupled into R_4 in the zero chirp and positive chirp cases while partly coupled into R_4 in the negative chirp case. At the same time, we find that the negative chirp makes the first-ejected fundamental soliton with a wider spectral range and a narrower temporal delay in contrast to the cases of zero chirp and positive chirp, which result from the fact that the fundamental soliton tunnels from R_2 to R_4 in the form of the transferred DWs. More importantly, the soliton frequency is continuously red-shifted in the presence of intra-pulse Raman scattering, which implies the continuous decrease in the group velocity in the anomalous dispersion regime. Therefore, even though the spectra of red-shifted solitons are separated from those of the DWs, they may still overlap in the time domain. As shown in Fig. 4, when the GVM condition between fundamental solitons and DWs is satisfied, fundamental solitons can capture the B-DWs at the leading edge under the effect of FWM. The intensity of the captured wave is associated with the intensity of the fundamental solitons formed in R_4. Compared with zero chirp and positive chirp, negative chirp suppresses the SST effect, which makes the first-ejected fundamental soliton transform into the form of the transferred DWs, and thus generating a smoother SC, as shown in the output spectra. In a word, the spectral range and flatness can be manipulated to a large extent by controlling the initial chirp on the SST, which provides an opportunity to obtain a much broader and smoother SC with an optimal chirp value.

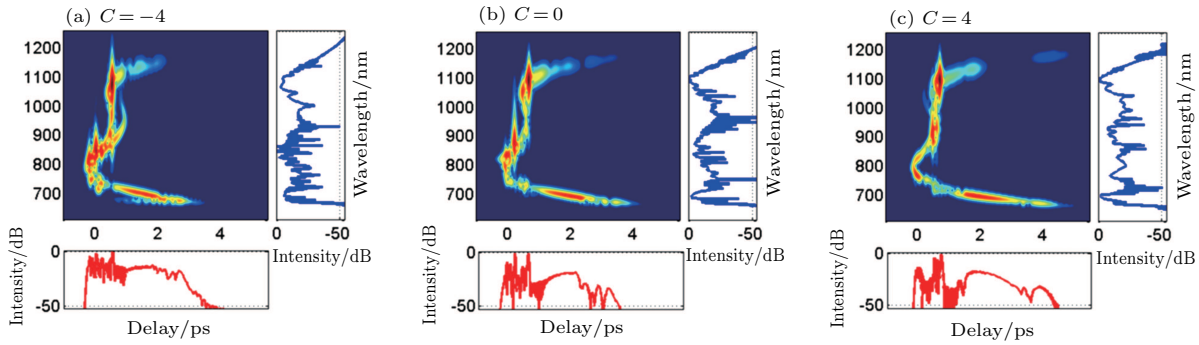


Fig. 4. (color online) Spectrograms with different initial chirps at the output of the PCF with three ZDWs: (a) $C=-4$, (b) $C=0$, and (c) $C=4$.

In order to have a closer look at how to manipulate the SC based on the influence of initial chirp on the SST, the spectrogram traces at three different propagation distances are plotted in Fig. 5. In the initial stage of pulse evolution, the SPM plays a dominant role in spectral broadening. The shape of the broadened spectrum mainly depends on the initial pulse shape and chirp value. When the propagation distance increases to 2 cm, the input pulse is broadened almost symmetrically in both spectral and temporal domains in the zero chirp case. Nevertheless, for negative chirp and positive chirp, the broadening of the input pulse becomes highly asymmetric in both spectral and temporal domains. Besides, positive chirp makes the spectrum broaden at a quicker speed and the oscillatory structure less pronounced in contrast to the cases of zero chirp and negative chirp.

When the propagation distance increases to 4 cm, the fission of the higher-order soliton takes place due to Raman effects, generating a series of fundamental solitons accompanied by B-DW radiation. However, only a fundamental soliton is ejected, resulting from the SRS effect, whose energy transfers from R_2 to R_4 under the effect of SST. With the increase in initial chirp, the SST effect occurs at a faster speed, resulting in the first-ejected fundamental soliton with a higher intensity and a larger red-shift. The positive chirp makes more energy transfer from the fundamental soliton in R_4 to the B-DWs in R_1 than zero chirp and negative chirp. As for negative chirp, the asymmetry of broadening is enhanced in both spectral and temporal domains.

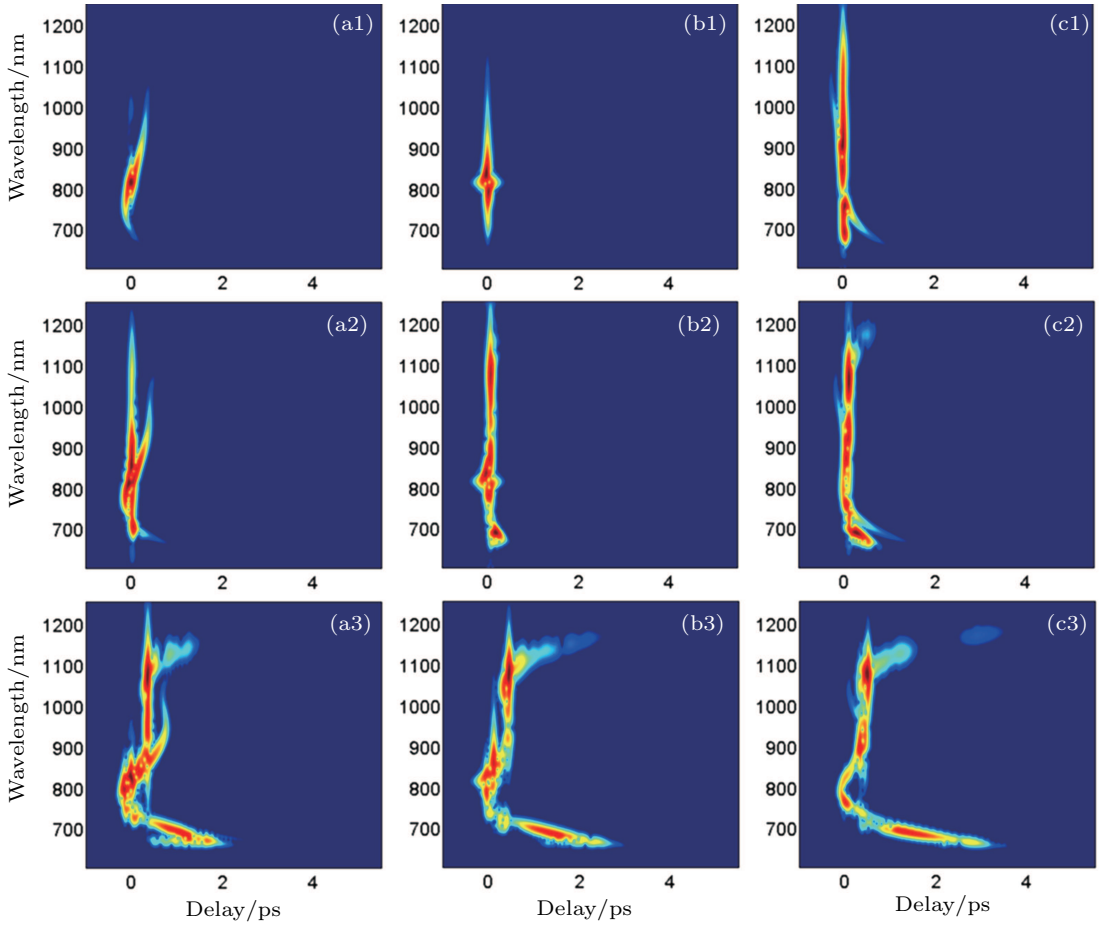


Fig. 5. (color online) Numerical spectrogram traces of pulse with different chirps and different propagation distances: (a1) $C = -4$, $z = 2$ cm, (a2) $C = -4$, $z = 4$ cm, (a3) $C = -4$, $z = 12$ cm, (b1) $C = 0$, $z = 2$ cm, (b2) $C = 0$, $z = 4$ cm, (b3) $C = 0$, $z = 12$ cm, (c1) $C = 4$, $z = 2$ cm, (c2) $C = 4$, $z = 4$ cm, and (c3) $C = 4$, $z = 12$ cm.

When the propagation distance increases to a certain value, the second fundamental soliton is ejected into R_2, whose intensity is lower than the first one. From Figs. 5(a3)–5(c3), we can see that the red-shift rate of the fundamental soliton is gradually improved with the increase in chirp value. However, due to the adverse effect of negative chirp on SSFS, the first-ejected fundamental soliton has not yet been fully coupled into R_4 to form a new soliton in Fig. 5(a3). When transferring through R_3, the fundamental soliton is compressed in the time domain while expanded in the spectral domain, which leads to the generation of SC with a smoother spectrum. In addition, the intensity of B-DWs is closely related to that of the fundamental soliton, and thereby enhanced with the increase in initial chirp. When the GVM condition between solitons and DWs is met, these fundamental solitons can capture B-DWs at the leading edge under the effect of FWM.

From the analysis above, one finds that the positive chirp can accelerate the emergence of the SST effect, which makes the SC have a broader spectral range by enhancing both the red-shift of the fundamental soliton and the blue-shift of DWs. Meanwhile, negative chirp can suppress the SST effect, which makes the SC have a smoother spectrum due to the spectral broadening of the first-ejected fundamental soliton when transmitting through R_3.

In the process of pulse evolution, one needs to take into account the influence of not only initial chirp but also the chirp induced by both GVD and SPM on temporal and spectral broadening. When a femtosecond pulse is launched in the anomalous dispersion regime, the dispersion-induced chirp is negative while SPM-induced chirp is positive. In order to further present the initial chirp effect on pulse evolution, figure 6 shows the temporal broadening factor and spectral broadening with different initial chirp values as a function of normalized distance. The temporal broadening factor is defined as σ/σ_0, where σ_0 is the initial root mean square (RMS) width of the input pulse, and σ is the RMS width after propagating a distance z.[3] The normalized distance is defined as z/L_D, where z is the propagation distance, and $L_D = T_0^2/|\beta_2|$ is the dispersion length.[3,5] From Fig. 6(a), one can see that the broadening of the pulse is larger for a larger initial chirp value, which agrees well with the phenomena shown in Fig. 2. In Fig. 6(b), the SPM makes spectral broadening have a typical oscillatory structure. In contrast to negative chirp and zero chirp, positive chirp needs a shorter fiber length to arrive at the saturation broadening stage. In addition, spectral broadening is larger for a larger initial chirp value. As one can see in Figs. 6(a) and 6(b), the initial chirp plays an important role in both temporal and spectral evolution in the process of SC generation. There-

fore, one can obtain the desired SC spectrum by choosing the appropriate initial chirp parameters.

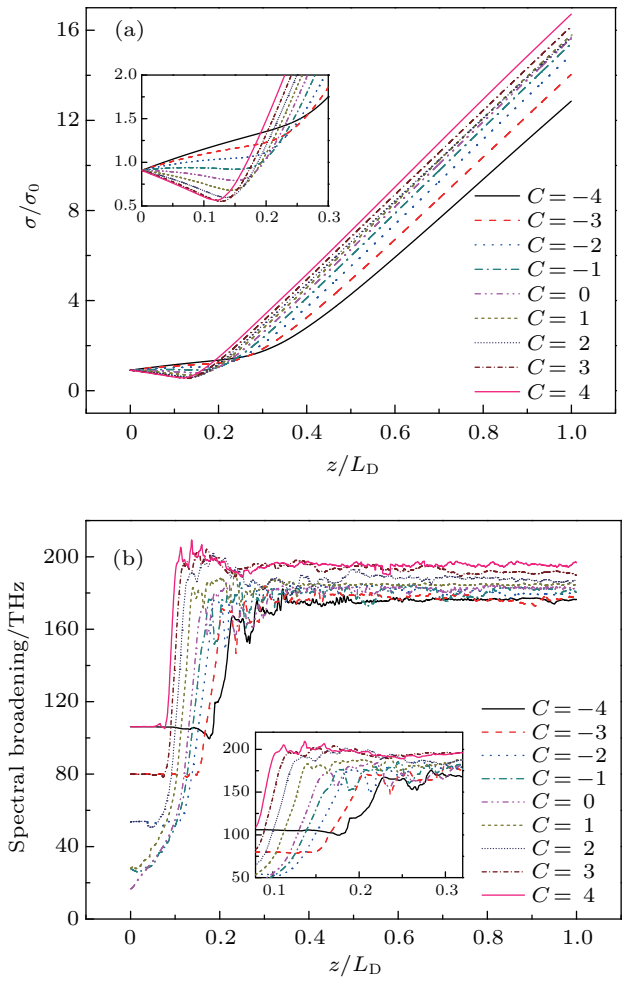


Fig. 6. (color online) (a) Temporal broadening factor and (b) spectral broadening with different initial chirp values as a function of normalized distance, with insets showing magnified corresponding positions.

4. Conclusion and perspectives

In this paper, we show that one can manipulate the SC based on the influence of chirp on SST in the PCF with three ZDWs. In order to better analyze temporal and spectral evolution, we illustrate the output spectrograms with different initial chirps. With the increase in initial chirp, the input pulse completes the initial broadening stage at a faster speed, and hence a series of fundamental solitons is ejected earlier, which facilitates the emergence of the SST effect. The SST effect makes the energy of the fundamental soliton continuously transfer from one anomalous dispersion regime to another. In this case, positive chirp can enhance the SST effect to make the SC have a much wider spectral range while negative chirp can suppress the SST effect to obtain a much smoother SC spectrum. In brief, initial chirp has an important influence on the SST effect when the femtosecond pulse propagates in the PCF with three ZDWs, which provides a new possibility to obtain a much broader and smoother SC in the future.

References

[1] Foster M A, Turner A C, Lipson M and Gaeta A L 2008 *Opt. Express* **16** 1300
[2] Dai C Q and Chen J L 2012 *Chin. Phys. B* **21** 080507
[3] Agrawal G P 2012 *Nonlinear Fiber Optics* (5th Edn.) (New York: Academic Press)
[4] Zhao S, Yang H, Zhao C and Xiao Y 2017 *Opt. Express* **25** 7192
[5] Dudley J M, Gentry G and Coen S 2006 *Rev. Mod. Phys.* **78** 1135
[6] Tsoy E N and Sterke C M d 2007 *Phys. Rev. A* **76** 043804
[7] Kibler B, Lacourt P A, Courvoisier F and Dudley J M 2007 *Electron. Lett.* **43** 967
[8] Belyaeva T, Serkin V, Hernandez-Tenorio C and Garcia-Santibanez F 2010 *J. Mod. Opt.* **57** 1087
[9] Guo H, Wang S, Zeng X and Bache M 2013 *IEEE Photon. Technol. Lett.* **25** 1928
[10] Stepniewski G, Klimczak M, Bookey H, Siwicki B, Pysz D, Stepien R, Kar A K, Waddie A J, Taghizadeh M R and Buczynski R 2014 *Laser Phys. Lett.* **11** 055103
[11] Knight J C 2003 *Nature* **424** 847
[12] Manili G, Tonello A, Modotto D, Andreana M, Couderc V, Minoni U and Wabnitz S 2012 *Opt. Lett.* **37** 4101
[13] Dupont S, Moselund P, Leick L, Ramsay J and Keiding S 2013 *J. Opt. Soc. Am. B* **30** 2570
[14] Lei D J, Dong H, Yang H, Wen S C, Zhang J G and Xu H W 2009 *Chin. Phys. Lett.* **26** 6
[15] Falk P, Frosz M H and Bang O 2005 *Opt. Express* **13** 7535
[16] Wang W B, Yang H, Tang P H and Han F 2013 *Acta Phys. Sin.* **62** 18 (in Chinese)
[17] Stark S P, Biancalana F, Podlipensky A and Russell P St J 2011 *Phys. Rev. A* **83** 3818
[18] Akhmediev N and Karlsson M 1995 *Phys. Rev. A* **51** 2602
[19] Poletti F, Horak P and Richardson D J 2008 *IEEE Photon. Technol. Lett.* **20** 1414
[20] Wang S, Guo H, Fan D, Bai X and Zeng X 2013 *IEEE Photon.* **5** 6100608
[21] Zhao S, Yang H, Chen N, Fu X and Zhao C 2015 *IEEE Photon.* **7** 7102709
[22] Neyra E, Videla F, Pérez-Hernández J A, Ciappina M F, Roso L and Torchia G A 2016 *Laser Phys. Lett.* **13** 115303
[23] Zhang H, Yu S, Zhang J and Gu W 2007 *Opt. Express* **15** 1147
[24] Fuerbach A, Miese C, Koehler W and Geissler M 2009 *Opt. Express* **17** 5905
[25] Valadan M, D'Ambrosio D, Gesuele F, Velotta R and Altucci C 2015 *Laser Phys. Lett.* **12** 025302
[26] Cheng C F, Wang X F and Shen B F 2004 *Chin. Phys. Lett.* **21** 10
[27] Xiao Y, Maywar D N and Agrawal G P 2012 *J. Opt. Soc. Amer. B* **29** 2958
[28] Corwin K L, Newbury N R, Dudley J M, Coen S, Diddams S A, Weber K and Windeler R S 2004 *Phys. Rev. Lett.* **90** 11
[29] Zhang Q, Takahashi E J, Müucke O D, Lu P and Midorikawa K 2011 *Opt. Express* **19** 7190
[30] Zhu Z and Brown T G 2004 *Opt. Express* **12** 689
[31] Blow K J and Wood D 1989 *IEEE J. Quantum Electron.* **25** 2665
[32] Hao Z, Zhao C, Wen J, Wen S and Fan D 2011 *Acta Opt. Sin.* **31** 75